Fully Kinetic Simulations of Radio Emission from a Propagating Electron Beam (SM35D-1996)

Tien Vo[1,3] (Tien.Vo@colorado.edu), Vadim Roytershteyn[2], and Cynthia Cattell[1]

[1] University of Minnesota – Twin Cities

[2] Space Science Institute

[3] University of Colorado - Boulder

Abstract

Fully kinetic PIC simulations are used to investigate how flare accelerated electron beams propagate over long distances while continually generating electromagnetic waves. The simulations describe the relevant linear and nonlinear kinetic processes from first principles and are performed in a large domain with open boundary conditions. The beam is injected from one side of the domain and experiences a rapid relaxation due to the action of instabilities over distances of tens of electron inertial lengths. However, only about 15% of the beam energy density is lost during this process. This enables the beam to propagate in a marginally stable state over long distances. Both fundamental and second harmonic emissions, signatures of nonlinear conversion processes, are observed. At large distances from the source, instabilities exist only in the front of the beam, unless the background plasma changes downstream.

I. Introduction

Type III radio bursts are produced as electrons accelerated by solar flares propagate out through the corona and into the solar wind. The standard theory for radio emission involves the conversion of Langmuir waves excited by electron beams via the bump-on-tail instability (see Fig. 1) [1].

Figure 1. Diagrams of nonlinear processes related to type III radio emission [2].

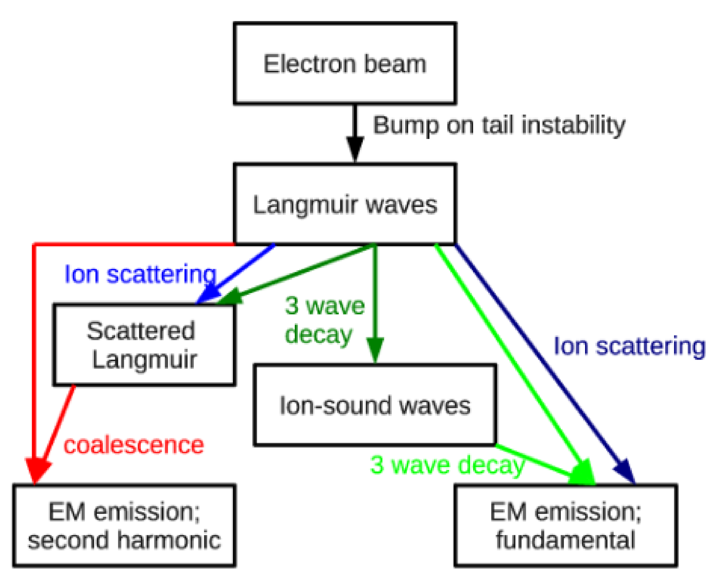

However, an issue with this picture is the so-called Sturrock's dilemma [3]. The beam propagation is in theory completely disrupted after a few kms by means of radio emission. Since signatures of type III emissions are observed at 1 AU, the instability needs to be finely balanced with the beam propagation so that electrons could travel far from the Sun.

To explain this, many models invoking contrasting processes have been proposed, for example, quasilinear vs strong turbulence description of interactions between various plasma modes [4,5]. The former proposes that the reabsorption of wave energy back into the stream may allow it to persist to large distances. The latter involves weak/strong turbulent processes that could shift the stream created waves out of resonance with the electrons fast enough to stabilize it.

In this study, we perform 2D PIC simulations of beam injection, propagation, and wave emissions and study the signatures relating to each model and their evolution in the simulation box.

II. Simulation parameters

- The dimensions of the simulation box (Fig. 2C) are 200 × 400 in electron inertial lengths. A Maxwellian beam is injected between the white arrows and moves across the box.
- Background parameters: $\omega_{pe}/\omega_{ce} = 20, T_e = 10T_i, v_{te} = 0.025c$.
- The injected beam has density $n_b n_0 = 10^{-3}$ and drift speed $V_b = 8v_{te}$.

III. Evolution of the beam-plasma system

Figure 2. Overview of beam-wave evolution in the simulation box.

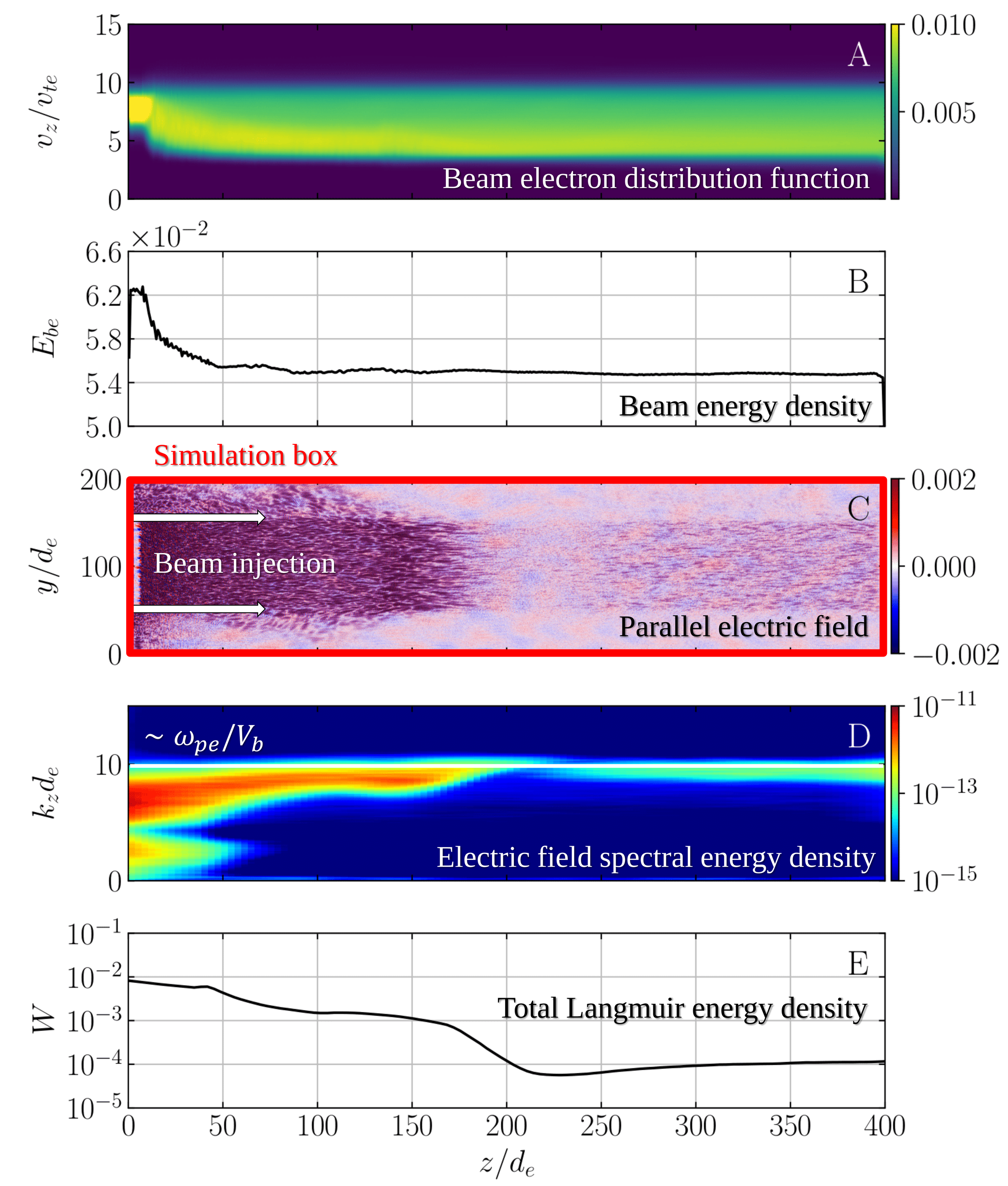

1. **Overview**: The beam in Panel A excites Langmuir waves in Panel C, whose wavevector is consistent with the bump-on-tail instability, as shown in the spectrogram in Panel D.
2. **Beam evolution**: In Panel A, the beam plateaus shortly after being injected ($z/d_e \geq 50$) and reaches a quasi-steady state where no further energy is lost to the instability in Panel B (see also Fig. 3). It only loses ~15% of the initial energy.
3. **Wave evolution**:
   - In Panel C, wave pileup occurs near the injection site, while the instability continues to operate only at the beam front downstream.
   - Some reabsorption occurs in between, resulting in a quiescent region separating these two regions of different intensity in wave activities.
   - In Panel E, only the strongly piled-up waves near the injection site ($z/d_e \leq 50$) exceed the threshold for turbulent processes, while the waves downstream evolve quasi-linearly.

Figure 3. Local electron distribution at 5 locations (colored) in the simulation box.

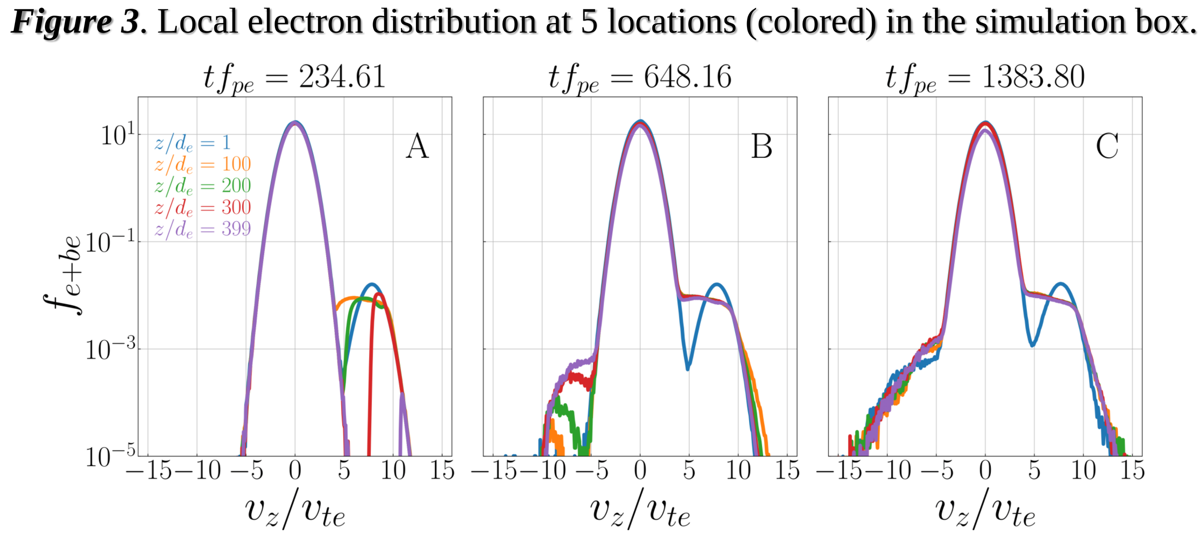

IV. Nonlinear processes

- Waves participating in classic 3-wave interaction processes are observed (see Fig. 4 & 5).
- Signature of the modulational instability connected to strong turbulence is observed in Fig. 4D (spectrogram taken near the injection site). The signature diminishes downstream, consistent with the wave energy density in Fig. 1E.

Figure 4. Spectral energy density in perpendicular/parallel wavenumber (k_y/k_z) vs frequency space. Panel A & B: Electromagnetic field. Panel C: Low frequency magnetic field. Panel D: Ion density.

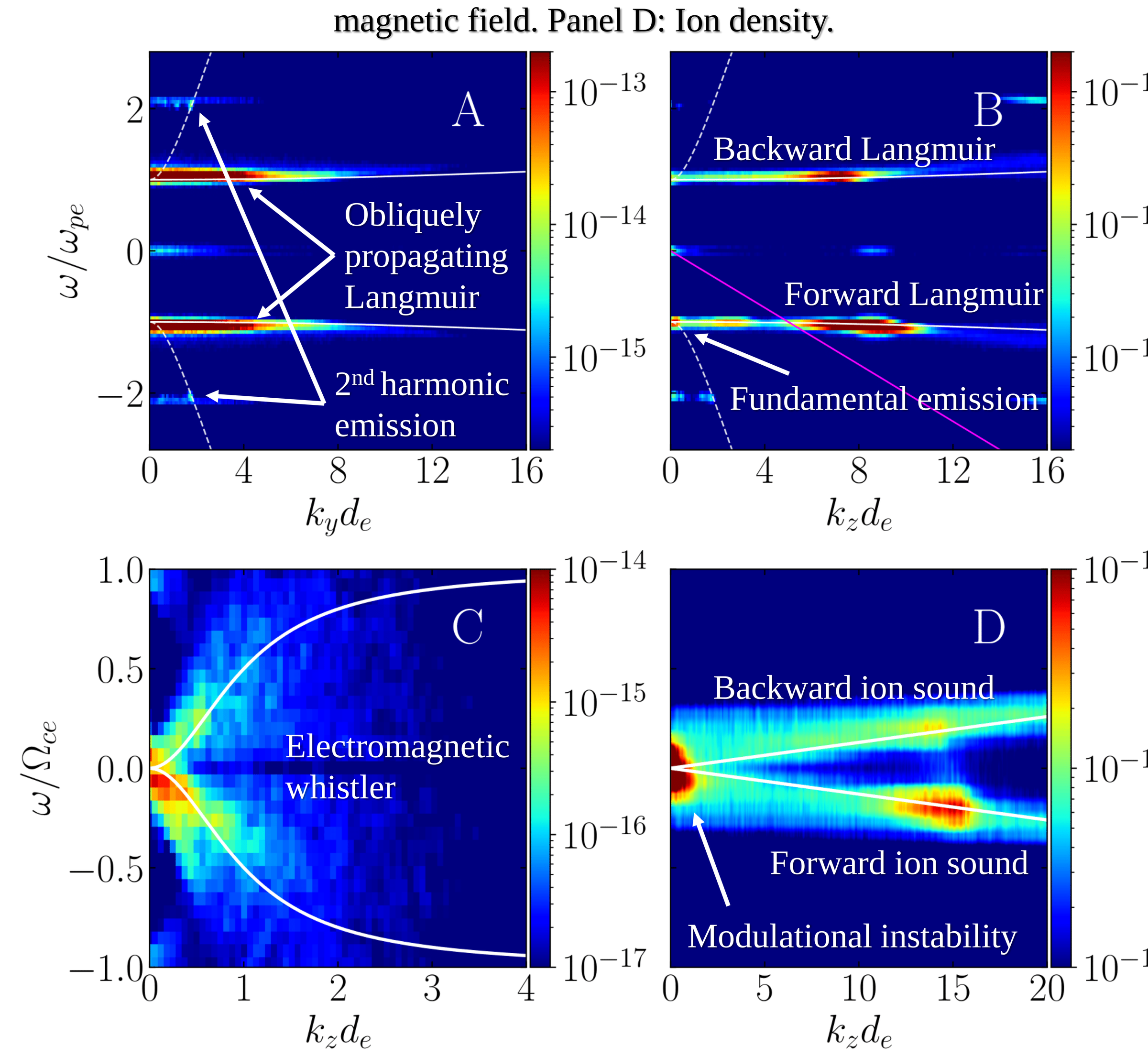

Figure 5. Spatiotemporal evolution of forward propagating Langmuir waves (A), backscattered Langmuir waves (B), and fundamental (C) and second harmonic (D) emissions. The color shows the local spectral energy density.

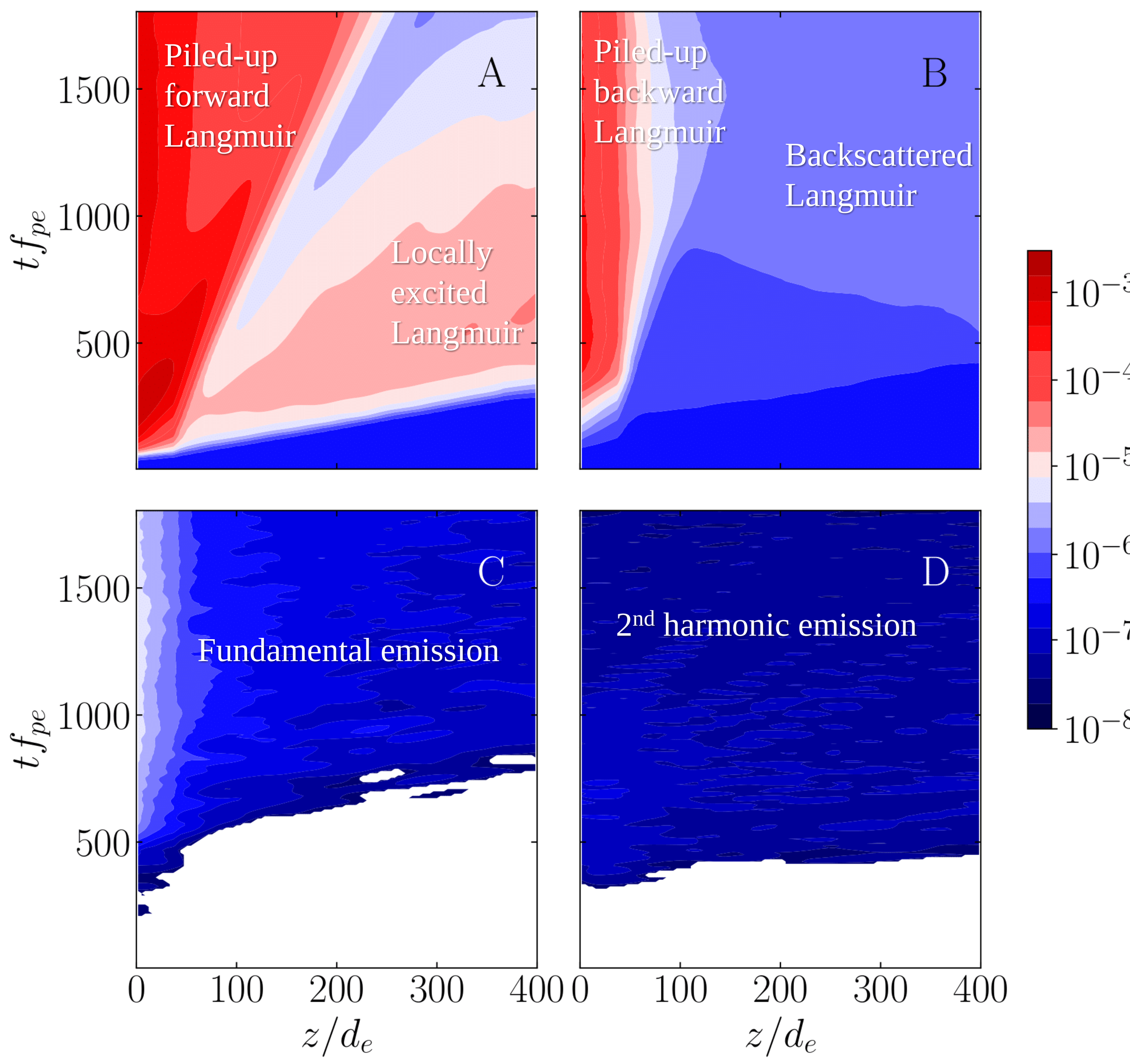

V. Discussions

- Most previous PIC studies of this type [6,7] used periodic boundary conditions, which imposes a ***uniformly strong coupling*** between the beam and the excited waves. However, as seen in our simulation, ***the beam quickly decouples from the waves and stabilizes***, leaving the instability only active at the front of the beam, while the rest of it plateaus. ***Thus, the escaping beam loses only a fraction of its initial energy and propagates in a marginally stable state, but it can become unstable again due to background temperature and/or density variations*** at larger heliospheric distances (see Fig. 6). The energy loss of the beam after the initial relaxation is ***consistent with that of quasi-linear evolution*** [8].

Figure 6. Linear stability analysis with varying temperature (A, B) and varying density (C, D).

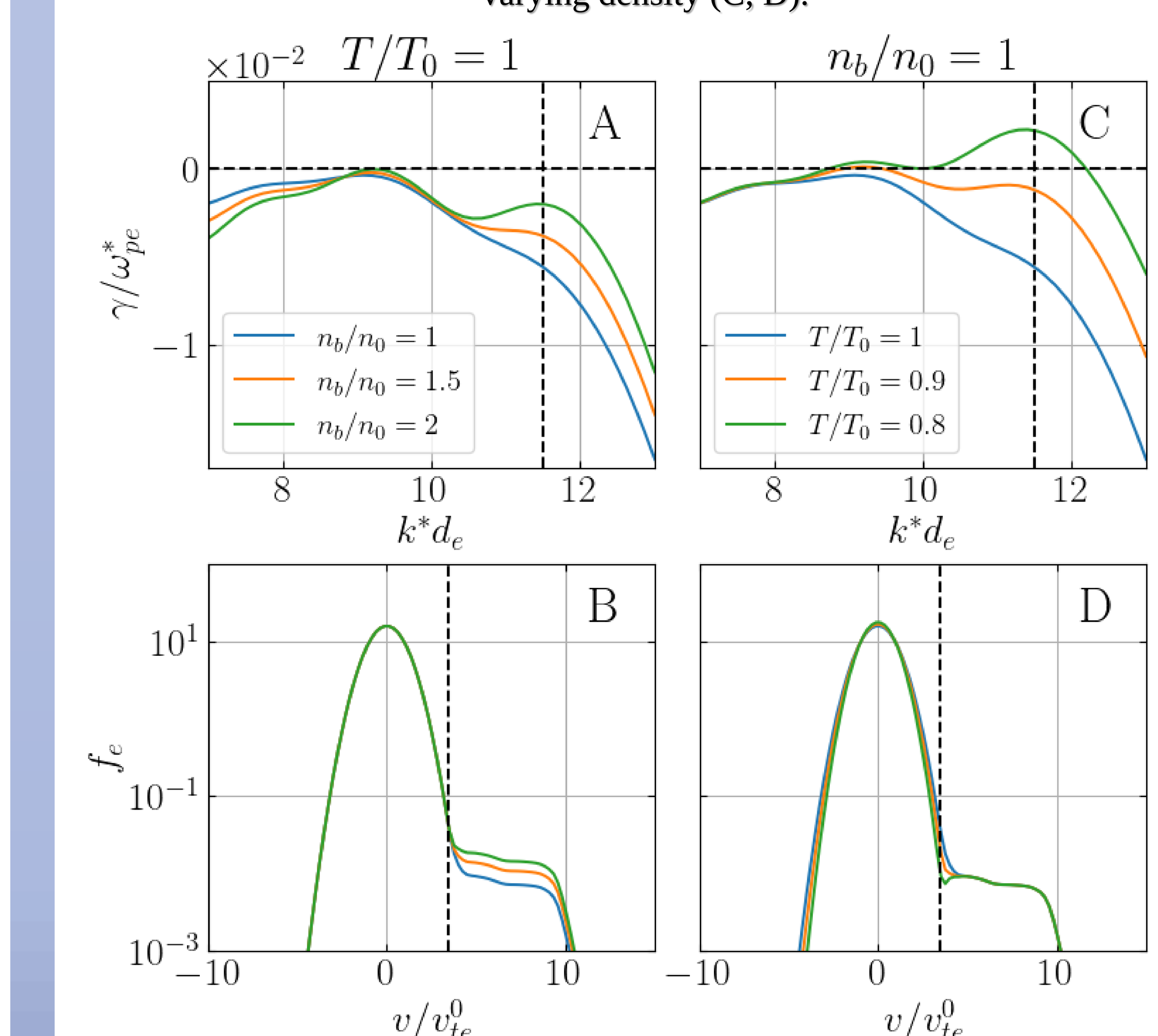

- In the context of type III bursts, weak/strong plasma turbulence theories have been investigated with simulations [9,10,11]. ***Although our model favors the quasi-linear evolution of the downstream beam***, ***signatures of turbulences are also observed*** due to the strong wave activities near the injection site.

References

[1] Robinson, P. A. et al. 1994, ApJ, 422, 870
[2] Reid, H. A. S. & Ratcliffe, H. 2014, RAA, 14(7), 773-904
[3] Sturrock, P. A. 1964, The Physics of Solar Flares, 357
[4] Zaitsev, V. V. et al. 1972, Solar Physics, 24, 444-456
[5] Papadopoulos, K. et al. 1974, ApJ, 190:175-185
[6] Thurgood, J. O. & Tsiklauri, D. 2015, A&A, 584, A83
[7] Henri, P. et al. 2019, JGR: Space Physics, 14, 1475
[8] Magelssen, G. R., & Smith, D. F. 1977, Solar Physics, 55, 211
[9] Che, H. et al. 2017, PNAS, 114, 1502
[10] Kontar, E. P. 2001, A&A, 375, 629
[11] Li, B. et al. 2006, PoP, 13